Bioconjugate Chemistry

Article

pubs.acs.org/bc

# Cell Penetrating Peptide (CPP)-Conjugated Desferrioxamine for Enhanced Neuroprotection: Synthesis and in Vitro Evaluation

Dibakar Goswami,[†] M. Teresa Machini,[‡] Daniel M. Silvestre,[†] Cassiana S. Nomura,[†] and Breno Pannia Esposito*[,†]

[†]Departamentos de Química Fundamental e de [‡]Bioquímica, Instituto de Química, Universidade de São Paulo, Av. Lineu Prestes 748, 05508-000, São Paulo, Brazil

Supporting Information

**ABSTRACT:** Iron overload causes progressive and sometimes irreversible damage due to accelerated production of reactive oxygen species. Desferrioxamine (DFO), a siderophore, has been used clinically to remove excess iron. However, the applications of DFO are limited because of its inability to access intracellular labile iron. Cell penetrating peptides (CPPs) have become an efficient delivery vector for the enhanced internalization of drugs into the cytosol. We describe, herein, an efficient method for covalently conjugating DFO to the CPPs TAT(47−57) and Penetratin. Both conjugates suppressed the redox activity of labile plasma iron in buffered solutions and in iron-overloaded sera. Enhanced access to intracellular labile iron compared to the parent siderophore was achieved in HeLa and RBE4 (a model of blood-brain-barrier) cell lines. Iron complexes of both conjugates also had better permeability in both cell models. DFO antioxidant and iron binding properties were preserved and its bioavailability was increased upon CPP conjugation, which opens new therapeutic possibilities for neurodegenerative processes associated with brain iron overload.

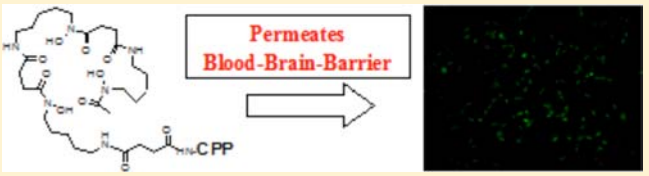


## INTRODUCTION

Iron, particularly important for the synthesis of proteins responsible for oxygen transport, electron transfer, and redox processes,[1] is absorbed in the duodenum from dietary sources, transported by transferrin across the cells and bloodstream, and stored in ferritin.[2] No dedicated mechanism of excretion of excess iron exists; hence, iron absorption is tightly regulated, both systemically and also in individual cells, to maintain body homeostasis.

There are instances[3] where excess iron can access organs and tissues through different routes, causing iron overload. Iron overload results in accumulation of "free" and highly reactive iron in the blood plasma (Labile Plasma Iron, or LPI, the redox-active component of Non-Trasferrin Bound Iron, NTBI) or in the cytosol.[4] These are the primary sources of potentially toxic redox active iron, which is responsible for generating oxidative stress and cell death via lipid peroxidation, and oxidation of amino acids, proteins, and DNA.[5−7]

The central nervous system is particularly affected by iron overload,[8] and evidences associated iron overload with brain degeneration leading to processes including Alzheimer's and Parkinson's diseases.[9a−d] Studies also reveal that elderly people with high brain iron levels perform badly in cognitive tests.[9e] Apart from iron, other metals, e.g., aluminum, copper, and zinc, when present with iron, also increase the production of ROS.[10a−c] Hence, an iron chelator with high blood-brain-barrier (BBB) permeability, high affinity for iron, and ability to chelate other metals can be a potential candidate for the chelation therapy of brain iron overload.[10d]

Overall, an "all-in-one" iron chelator for the treatment of iron overload should target both plasmatic and cytosolic iron. Chelators, e.g., desferrioxamine, deferasirox, and deferiprone are being used in clinical practice.[11] Among these, desferrioxamine-B (DFO), a hexadentate and highly selective iron chelator with considerable affinity for aluminum and zinc,[12a] has been the most thoroughly studied,[12b] and was the first drug clinically used for the treatment of iron overload diseases.[11,13] Although DFO has shown antioxidant,[14a] antiproliferative, and antitumor activities,[14b] its poor bioavailability (due to its high hydrophilicity and high molecular weight[11a]) renders the drug to always be administered as a continuous intravenous infusion, making the treatment expensive and uncomfortable.[15]

Although DFO has shown appreciable anti-Alzheimer activity in one clinical trial,[16] its low BBB permeability has restricted its use for the treatment of neurodegenerative diseases.[17] Recently, nanoparticle−DFO conjugates[10d,18] and also several other modified analogs of DFO, e.g., with peptides,[19a] ferrocene,[19b] fluorophores,[19c−e] hydroxypyridinonate, or catechoyl derivatives,[19f−h] derivatives of adamentane or deferasirox,[19i,j] hydroxyethyl starch,[19k] or nonamide and C-terminal modified analogs,[19l] have also been evaluated for iron removal in several ways. Extensive research has also been carried out in the past decade on the design, synthesis, and evaluation of other iron chelators or their conjugates in order to attain better BBB

**Received:** September 8, 2014
**Revised:** October 2, 2014
**Published:** October 9, 2014





dx.doi.org/10.1021/bc5004197 | *Bioconjugate Chem.* 2014, 25, 2067−2080

**Scheme 1**

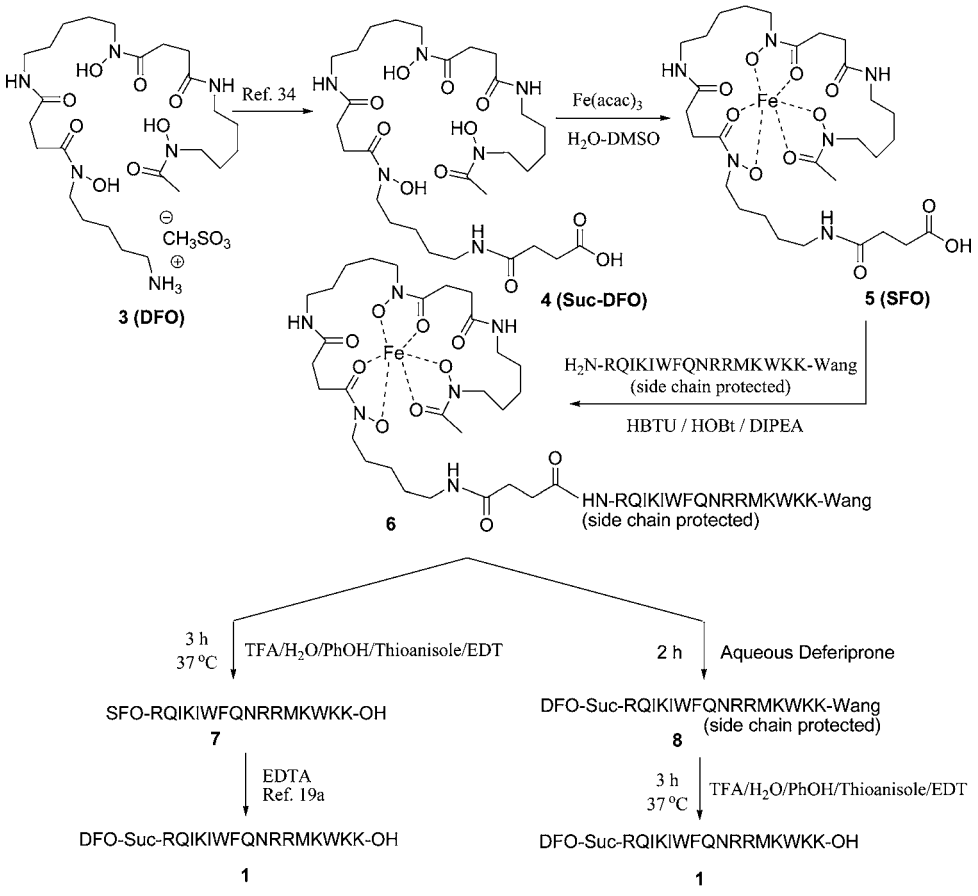


permeability.[20] For example, 5-[*N*-methyl-*N*-propargylaminomethyl]-8-hydroxyquinoline containing both neuroprotective and BBB-permeable iron chelator moieties,[21] a glucose-deferiprone adduct,[22] and some peptide derivatives with iron chelating properties and antioxidant activities have also been developed[23] for this purpose. However, all these BBB-permeable compounds are bidentate ligands (forming 3:1 chelates with iron) and are likely to be toxic,[24] whereas hexadentate iron chelators have generally lower toxicity,[25] albeit with low BBB permeability. Hence, there is enormous interest in designing new iron chelators based on the hexadentate ligand DFO bound to an "inert" BBB carrier, so that the properties of the conjugate may be tuned as desired, retaining the iron-binding characteristics of DFO.

In this context, we envisaged that cellular delivery of DFO through attachment to a cell penetrating peptide (CPP) can be very advantageous. Several biologically relevant molecules have been subjected to targeted cell delivery via either covalent or noncovalent conjugation with a CPP,[26a−d] leading to better pharmacokinetics and cell penetration.[26e] CPPs are advantageous as delivery vectors owing to their low cytotoxicity and high permeability to a variety of cells.[27] Among various examples of natural and synthetic CPPs, TAT(47−57)[28] and penetratin[29] have been the foundation of all the CPPs, and attracted attention as both are able to enhance BBB permeability of several bioactive molecules.[30,31] Herein, we report a new synthetic route to synthesize DFO−CPP conjugates, their iron binding abilities, their antioxidant properties, and their cell permeability compared to the parent siderophore.

## RESULTS

**Synthesis and Characterization of Peptides and Peptide−DFO Conjugates.** *Penetratin and TAT(47−57) Peptides.* Penetratin [RQIKIWFQNRRMKWKK] peptide was synthesized manually by solid-phase methodology on Fmoc-Lys(Boc)Wang resin (0.1 g, 0.56 mmol/g) using the Fmoc/$^t$Bu strategy and protocols routinely used in our laboratories.[32] The amino acid side-chain protecting groups were trityl (Trt) for Asn and Gln, 2,2,4,6,7-pentamethyl dihydrobenzofuran-5-sulfonyl group (Pbf) for Arg, and *tert*-butyloxycarbonyl (Boc) for Lys and Trp. Fmoc deprotections, in the initial step of peptide assembly on resin and also after each amino acid coupling, were performed using a 20% piperidine in DMF solution for 10 min. Except for Asn and Gln couplings on the growing peptide resin, the amino acid couplings were performed by dissolving Fmoc-amino acid, DIC, and HOBt (1:1:1) in a minimal amount of DCM-DMF (1:1, v/v), and using 2.5 molar excess relative to the resin capacity. For couplings of Asn and Gln derivatives, HBTU/HOBt/DIPEA were employed after dissolving in a minimal amount of DMF in a ratio of 4:4:9 relative to the resin capacity. The reactions proceeded at room temperature (RT) for 60 min under mechanical shaking. The peptidyl-resin was washed (DMF 2 × 1 min, DCM 2 × 1 min). The efficiency of Fmoc deprotection and coupling reactions were checked by the ninhydrin test.[33]


dx.doi.org/10.1021/bc5004197 | *Bioconjugate Chem.* 2014, 25, 2067−2080

**Scheme 2**

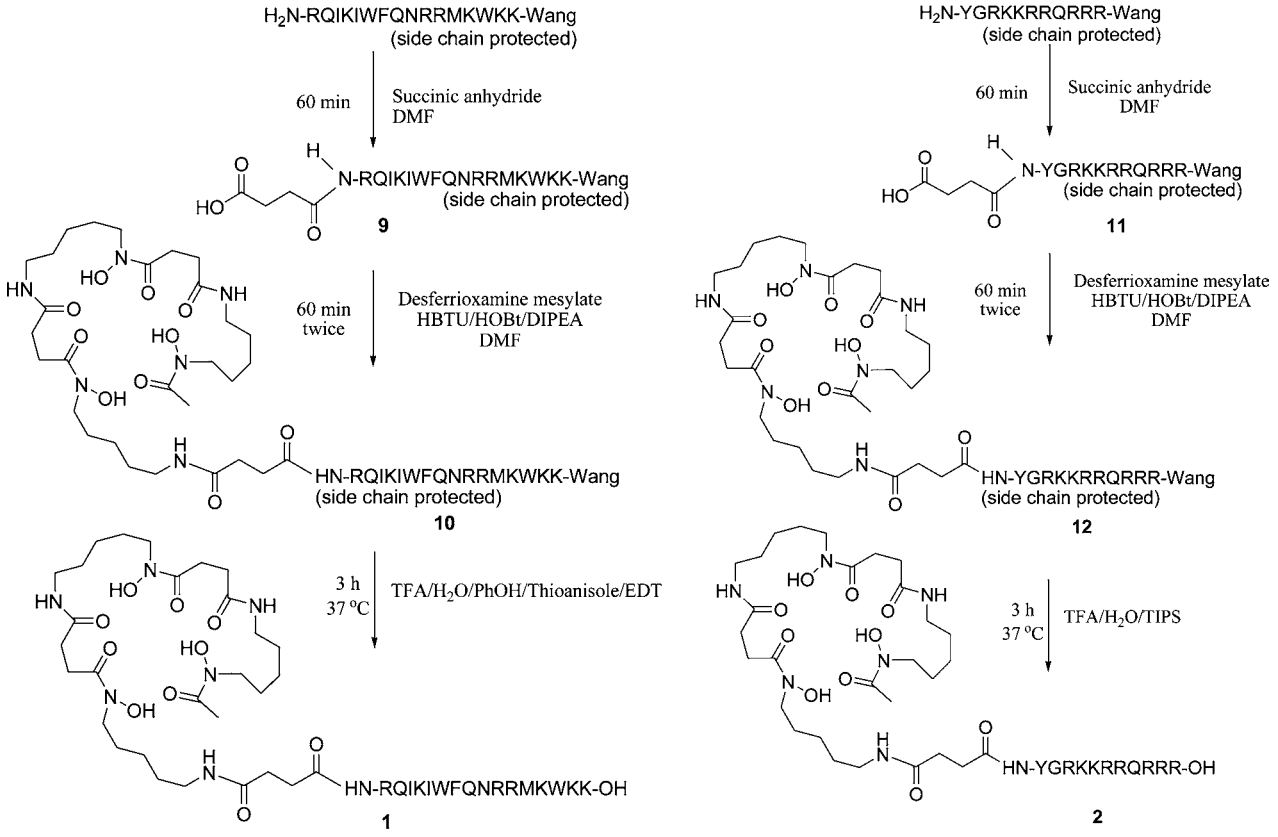


After total peptide assembly on resin, the product was cleaved from it at 37 °C for 3 h with 0.84 mL TFA containing 0.06 g PhOH, 0.04 mL distilled water, 0.04 mL thioanisole, and 0.02 mL EDT as scavengers. The crude product was precipitated by sequential additions and removals of dry diethyl ether, dissolved in 0.1% aq TFA, isolated by filtration, and freeze–dried.

TAT(47–57) (YGRKKRRQRRR) peptide was synthesized manually on Fmoc-Arg(pmc)-Wang resin (0.1 g, 0.61 mmol/g) using the same strategy and protocols. The amino acid side-chain protecting groups were Trt for Gln, Pbf for Arg, Boc for Lys, and *tert*-butyl ($^t$Bu) for Tyr. Similarly to penetratin-Wang resin, peptide cleavage from resin and full deprotection was carried out in the mixture of TFA and scavangers as described above.

*Synthesis of Peptide–Desferrioxamine Conjugates.* In an endeavor to find out the best synthetic route, conjugation of the peptides to DFO was accomplished in three possible ways (Scheme 1).

First (Method 1a, Scheme 1), DFO mesylate (**3**) was reacted with succinic anhydride according to a reported procedure[34] to provide succinyl-DFO (**4**). Compound **4**, containing a free carboxyl group required for reaction with the free N-$\alpha$-amino group of the peptide-resin, was further converted to succinyl ferrioxamine (SFO, **5**) by mixing a DMSO solution of **4** with stoichiometric amount of aqueous Fe(acac)$_3$, and thereafter removing the solvents under vacuum.[19a] Reaction of **5** with the N-$\alpha$-amino group of the side-chain protected peptide-Wang resin (0.1 g) to get side-chain protected SFO-peptide-Wang resin (**6**) was achieved after two consecutive acylation reactions in DMF containing using HBTU/HOBt/DIPEA in DMF in a ratio of 4:4:9 relative to the resin capacity (RT, 120 min).

Conjugate **6** was cleaved from the resin and fully deprotected to get SFO–peptide conjugate (**7**) by incubation in 0.84 mL TFA with 0.06 g PhOH, 0.04 mL distilled water, 0.04 mL thioanisole, and 0.02 mL EDT at 37 °C for 3.5 h. Products were identified using LC-MS. Although we expected that in an acidic condition[35] conjugate **6** would lose its iron to give **1** directly, it did not happen. Increasing the reaction time from 3 to 5 h led to a mixture of conjugates **7** and **1** (as indicated by LC-MS), whereas an overnight reaction yielded a complex mixture of byproducts. The crude product **7** was precipitated by dry diethyl ether, dissolved in 0.1% aq TFA, and freeze–dried. The major component was characterized as conjugate **7**; the minor component (~30%, as calculated from LC-MS) was its methionine-oxidized form. The crude conjugate **7** was then demetaled according to a reported method[19a] allowing for the isolation of the metal free crude DFOSuc-penetratin conjugate (**1**) in a very poor yield (0.008 g).

Alternatively (Method 1b, Scheme 1), the resin bound SFO–penetratin conjugate (**6**, as prepared above, 0.1 g) was demetaled to give conjugate **8** by stirring in an aqueous solution of deferiprone (10 mM), which has a higher effective stability constant with iron.[36] After 2 h of stirring, the resin beads decolorized, and the aqueous solution turned red, indicating the transfer of iron from the conjugate **6** to deferiprone. The metal-free DFOSuc-peptidyl resin (**8**) was washed (2 × $H_2O$, 3 × MeOH), cleaved from the resin, and fully deprotected to get DFOSuc-peptide conjugate (**1**) by incubation in 0.84 mL TFA with 0.06 g PhOH, 0.04 mL


dx.doi.org/10.1021/bc5004197 | *Bioconjugate Chem.* 2014, 25, 2067–2080

distilled water, 0.04 mL thioanisole, and 0.02 mL EDT at 37 °C for 3 h. Products were identified by LC-MS. Conjugate **1** was precipitated, isolated, and characterized as described above, again with a poor yield (0.012 g), along with a minor component (~20%, as calculated from LC-MS) corresponding to its methionine-oxidized form.

All the methods described above are indirect and require temporary protection of the hydroxamates by iron chelation, which then needs to be removed. We envisaged that direct conjugation of DFO to the peptides could give higher yields and simplify the process. Toward this, we modified a reported protocol.[37] In this method (Method 2a, Scheme 2), the free $\alpha$-amino group of the side-chain protected peptidyl-resin (0.1 g) was stirred with a solution of succinic anhydride (10 equiv higher than the resin capacity) in a minimal amount of DMF for 60 min at RT. In contrast to a literature report,[37] the use of DIPEA in this step led to unwanted side reactions, and eventually less or no yield of the desired product. Acylation efficiency was monitored by the ninhydrin test.[33] The resulting succinyl-peptidyl resin (**9**) was coupled to DFO using HBTU/HOBt/DIPEA in DMF in a ratio of 4:4:9 relative to the resin capacity for 60 min at RT. The reaction was repeated to ensure its completion, which was verified by placing a few resin beads in a dilute $FeCl_3$ solution, which turned the beads brick red due to iron chelation. The resin was washed (2 × DMF, 2 × DCM, 2 × MeOH). The expected DFOSuc-peptidyl resin (**10**) was incubated in 0.84 mL TFA with 0.06 g PhOH, 0.04 mL distilled water, 0.04 mL thioanisole, and 0.02 mL EDT at 37 °C for 3 h to get conjugate **1**, which was precipitated as described above, and isolated with a higher yield (0.054 g), although with a minor contaminant (~20%, as indicated in LC-MS) corresponding to its methionine-oxidized form.

The higher yield of the DFOSuc–penetratin conjugate (**1**) prepared by Method 2a (Scheme 2) prompted us to use the same method for the preparation of DFOSuc-TAT(47–57) conjuagte (**2**). Side-chain protected TAT(47–57) peptide was prepared on Wang resin as described before. Succinic anhydride and subsequently DFO were reacted with the peptide (Method 2a, Scheme 2). However, cleavage of the crude peptide from the resin and full deprotection using the same cleavage cocktail resulted in a complex mixture of products. Incubation in an alternative cleavage cocktail (1 mL) containing TFA/Phenol/TIPS (95:2:3) for 3 h at 37 °C yielded the crude product that was precipitated by dry diethyl ether, dissolved in 0.1% aqueous TFA, and freeze–dried.

All the crude peptides and peptide conjugates were analyzed using LC/ESI-MS, which confirmed that the crude products contained the desired peptides or peptide-conjugates as major components. The peptides and the crude conjugates **1** and **2**, obtained by Method 2a and 2b (Scheme 2), were purified by semipreparative RP-HPLC[38] as described in the Experimental Section. After purification, the final targets were evaluated by analytical RP-HPLC analysis, LC-ESI/MS analysis (Supporting Information), and full acid hydrolysis/amino acid analysis of the hydrolyzates. The purities and peptide contents are summarized in Table 1.

The peptide contents of each purified peptides or conjugates were determined, so that concentrations could be calculated accurately prior to the biological assays and spectroscopic analyses.

**Competition Studies with Calcein.** Calcein, a fluorophore, is extensively used as a chemosensor for iron(III) in cells and biological fluids,[39a] and also to assess non-transferrin-bound iron (NTBI) in iron overloaded patients.[39b] Competition studies have been conducted in the presence of Fe(II), which is promptly oxidized upon coordination by calcein, with fast and stoichiometric quenching of fluorescence.[39c] Chelation of the ferric ion from calcein by the added chelators recovers the fluorescence.

**Table 1. Characterization of Peptides and Peptide–Desferrioxamine Conjugates**

| compound | purification yield/ peptide purity (%) | $[MH]^+$ calcd./ found | peptide content (%) |
|---|---|---|---|
| Penetratin | 12/>95 | 2246.7/2246.7 | 47 |
| TAT (47–57) | 27.8/>95 | 1559.8/1559.4[a] | 56 |
| Conjugate **1** | 20/>95 | 2889.4/2889.0[b] | 57 |
| Conjugate **2** | 23/90 | 2202.5/2202.6[c] | 44 |

[a]Peaks corresponding to $[M + n\text{TFA}]^+$, $n$ = 1–3, were also observed. [b]Peaks corresponding to $[M + \text{Mes}]^+$ were also observed. [c]Peaks corresponding to $[M + n\text{TFA} + \text{Mes}]^+$, $n$ = 1–3, were also observed.

At physiological pH, a plot of the calcein fluorescence recovery as a function of chelator concentration (Figure 1A,B) indicated that the binding profiles of both peptide-conjugates (conjugates **1** and **2**) were identical to that of DFO or Succinyl-DFO (Suc-DFO). At submicromolar levels, both **1** and **2** efficiently competed with calcein, indicating the high thermodynamic stability of their iron derivatives and their role in iron scavenging. If the iron is immobilized in stable, redox-inactive forms, these compounds might be useful in chelation therapy. The peptides alone lack strong metal binding

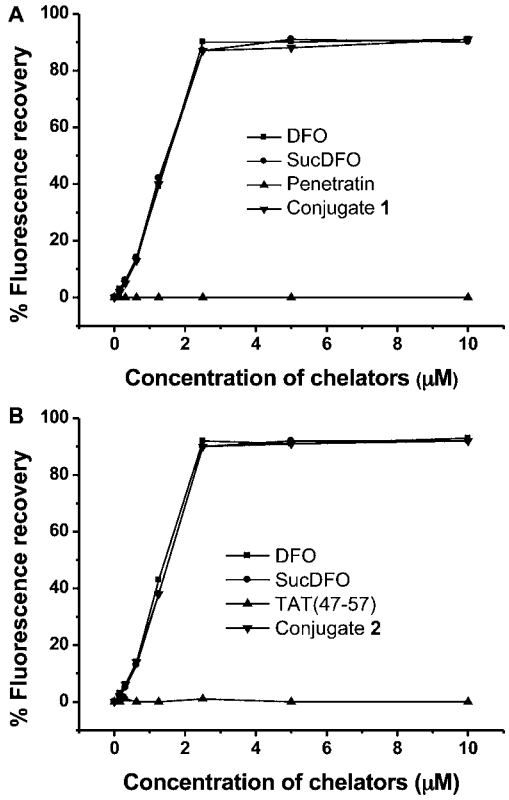


**Figure 1.** Fluorescence recovery (%) of calcein (2 $\mu$M) as a function of chelator concentration. (A) DFO, Suc-DFO, Penetratin peptide, and conjugate **1**; and (B) DFO, Suc-DFO, TAT(47–57) peptide, and conjugate **2** (results are the average of duplicate experiments and representative of at least two isolated experiments).


dx.doi.org/10.1021/bc5004197 | Bioconjugate Chem. 2014, 25, 2067–2080

sites and are positively charged, so therefore were not expected to compete with calcein for the iron. Accordingly, no fluorescence recovery was observed when the reaction was performed with them.

The experiment was also repeated at pH 5.5 and 8.1. Again, the conjugates showed iron binding profiles identical to the original siderophore DFO (data not shown). These results confirmed that any changes in peptide conformation due to changes in pH have no direct effect on the iron binding ability of the conjugates.

**Competition Studies with Fluorescein-Apotransferrin.** Transferrin, an iron binding protein in the serum, acts like a buffer, to maintain very low concentration of free iron in the body. Serum transferrin is responsible for the transport and delivery of iron to cells and tissues. In cases of iron overload, transferrin is highly saturated with iron. DFO, although a hexadentate ligand with higher affinity for iron than transferrin ($pM_{DFO}$ = 26.6 compared to $pM_{transferrin}$ = 23.6),[40a] is reported to be unable to remove iron from diferric transferrin even after several hours of incubation, since iron in transferrin is buried within the peptide framework of the protein.[40b]

For assessing the ability of the conjugates to remove iron from diferric transferrin, we prepared fluorescein apotransferrin (FlTf) by conjugating 5-DTAF with holo-transferrin, and subsequent dialysis against citrate (pH 5.5), according to a previously described method.[41] In our experiments (details in the Experimental Section), addition of FAS to FlTf quenched the fluorescence due to iron binding. However, subsequent addition of different concentrations of the chelators (DFO, **1** or **2**) did not lead to fluorescence recovery, indicating no iron transfer from transferrin to the chelators (data not shown). Similarly, addition of preformed iron complexes of DFO or conjugate **1** or conjugate **2** did not reduce the FlTf fluorescence, indicating no iron transfer from the iron:chelator conjugates to transferrin (data not shown).

However, when FAS was added to a mixture of FlTf and chelators (DFO, **1** or **2**), it was evident that the chelators have higher affinity toward iron (Figure 2). In the absence of chelators, all the iron was bound to FlTf, as indicated by rapid quenching of FlTf fluorescence (which reads as 100% FlTf-bound iron). However, with the increase in chelator concentration, the added iron preferably complexed with the chelator, leaving the FlTf free. This led to less or no quenching of the FlTf fluorescence. This behavior was expected keeping in mind the higher pM of DFO toward iron, as stated earlier. Once again, no difference was found between the conjugates and DFO, which indicated that peptide conjugation to DFO does not interfere with its iron-binding abilities.

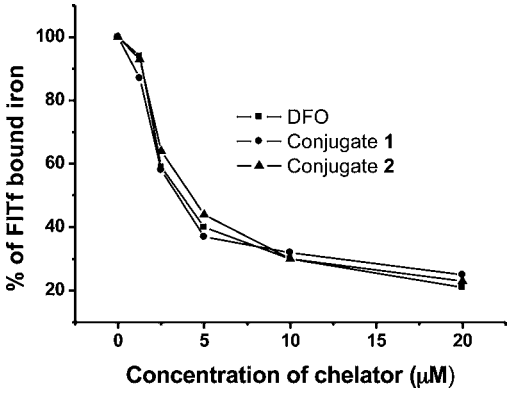


**Figure 2.** Percentage of FlTf-bound iron when FAS was added to FlTf in the presence of increasing concentrations of chelators. Results are the average of duplicates and representative of at least two isolated experiments.

**Antioxidant Activity.** Under physiological conditions, labile iron can generate ROS in the presence of low concentrations of ascorbate.[42] Increase in NTBI can lead to an unregulated cell permeation of iron, resulting in oxidative stress. Hence it is important to evaluate the candidate chelators for their ability to decrease LPI, the redox-active fraction of NTBI. DHR, an oxidant-sensitive dye, has been used extensively as a probe for LPI.[42,43] Oxidation of DHR caused by ROS produced by Fe/ascorbate leads to increase in fluorescence, the rate of which is directly proportional to the concentration of labile iron in the system. When a chelator is able to bind the metal through its six coordination positions with high stability, it halts ROS generation, which is measured as a decrease of the rate of DHR oxidation. Therefore, DHR oxidation rates are surrogates for the antioxidant activity of the chelators. Fe(NTA)/ascorbic acid solutions were chosen as a chemical model of LPI, and plasma samples from iron-overloaded patients were also studied (using methods detailed in the Experimental Section).

As shown in Figure 3A, Fe(NTA) alone causes a steady increase in the rate of DHR oxidation. A slight oxidation of DHR occurs even in the absence of added iron probably due to the presence of traces of this metal in the buffer. The

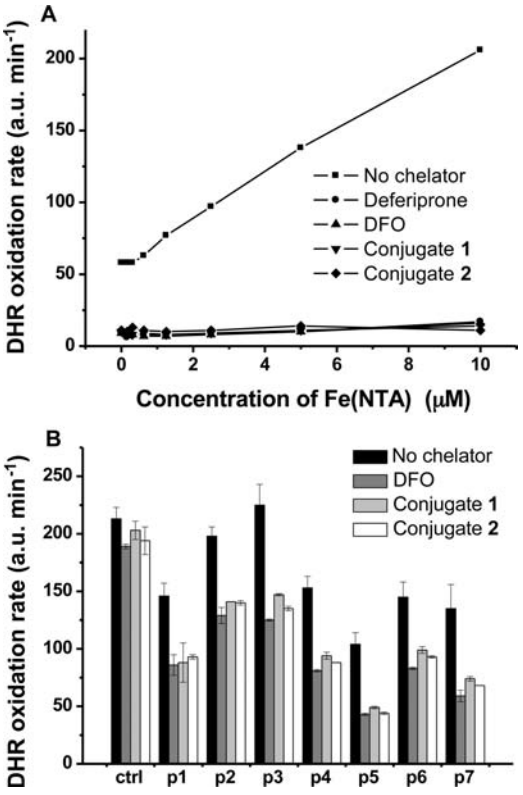


**Figure 3.** (A) Effect of the chelators (20 μM) on the rate of DHR oxidation catalyzed by iron/ascorbate in HBS/Chelex buffer (pH 7.4). (B) Sera from iron-overloaded patients (Pat#) treated with chelators (20 μM). (Control = serum from a normal subject without iron overload). Results are the average of duplicates and representative of at least two isolated experiments. a.u. = arbitrary fluorescence intensity.


dx.doi.org/10.1021/bc5004197 | Bioconjugate Chem. 2014, 25, 2067−2080

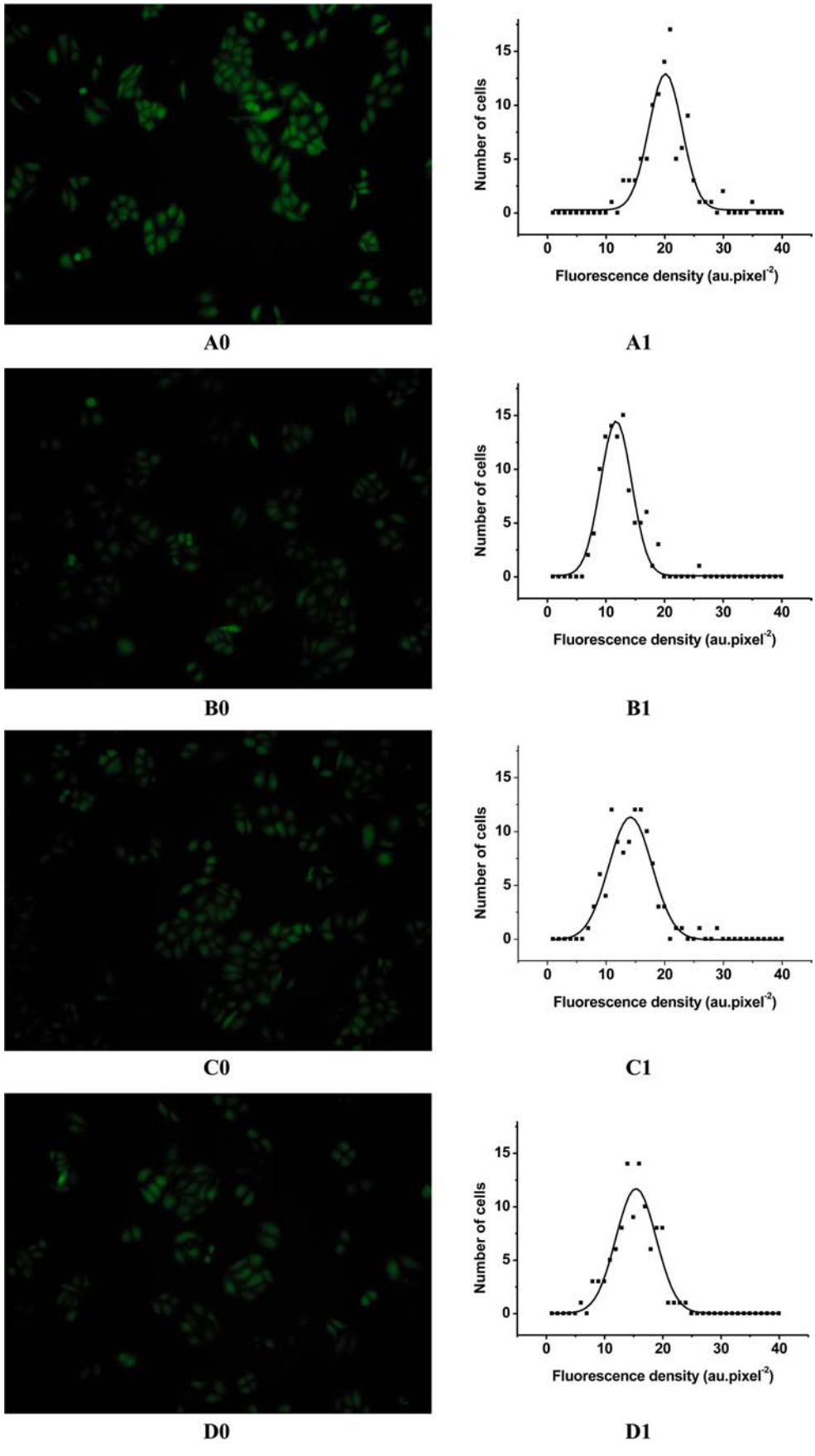


**Figure 4.** continued


dx.doi.org/10.1021/bc5004197 | *Bioconjugate Chem.* 2014, 25, 2067−2080

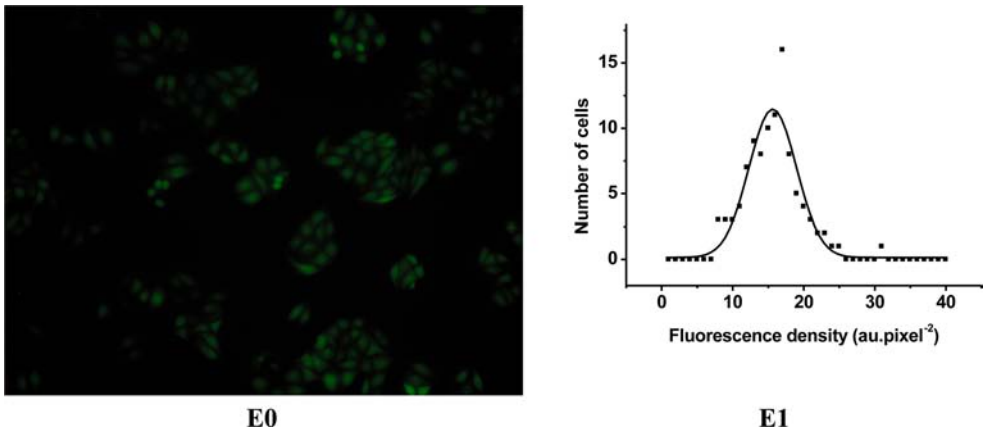


**Figure 4.** Effect of DFO, conjugate **1** and conjugate **2** on the fluorescence of calcein in HeLa cells. Cells were treated with buffer (A0), FAS/ascorbic acid (excess iron, B0), and excess iron plus DFO (C0), conjugate **1** (D0), or conjugate **2** (E0) (see Experimental Section). The graphs show cell population against fluorescence density for cells treated with buffer (A1, $x_c$ = 20.11 ± 0.22), after treatment with FAS/ascorbic acid (excess iron, B1, $x_c$ = 11.74 ± 0.14), and excess iron plus DFO (C1, $x_c$ = 14.15 ± 0.22), conjugate **1** (D1, $x_c$ = 15.41 ± 0.21), or conjugate **2** (E1, $x_c$ = 15.63 ± 0.21). a.u. = arbitrary fluorescence intensity.

antioxidant properties of **1** and **2** were substantiated by the virtually zero rate of DHR oxidation, comparable with the capacity of the parent siderophore DFO and the orally active iron chelator deferiprone. Conjugates **1** and **2** were also able to decrease LPI from the sera of iron-overloaded patients (Figure 3B) to a similar extent done by DFO. The effect of the peptides (penetratin and TAT(47−57)) was also evaluated, but as expected, they did not have any antioxidant properties under this experimental setup (data not shown).

**Cell Permeation Studies.** Finally, and most importantly, peptide conjugates **1** and **2** should be able to cross biological membranes, both free (to gain access to cytosolic iron) and iron-loaded (after binding the metal, the conjugate-iron complexes must exit the cell). To examine this point, two cell lines, viz., HeLa and RBE4, were chosen. HeLa and RBE4 cell lines were kindly provided by Prof. Mauricio Baptista (Universidade de São Paulo, Brazil) and Prof. Michael Aschner (Albert Einstein College of Medicine, USA), respectively. While HeLa cells represent a general cell-membrane model, RBE4, with the brain endothelium-specific expression of transport systems, has been accepted as a bona fide model of the blood-brain barrier (BBB).[44] The permeability of the conjugates was studied via fluorescence microscopy (details in the Experimental Section).

Cells were loaded with the probe calcein-AM, which displays fluorescence after esterase-catalyzed cleavage of the acetomethoxy group within the cell. When treated with excess iron, cell fluorescence was quenched, similarly to what was observed in solution. Any cell-permeant chelator should be able to regenerate this fluorescence signal. DFO, **1**, or **2** was then added to the culture medium and the fluorescence was again registered after 20 min. As observed, in both cell lines, iron-overloaded cells treated with **1** and **2** displayed a significant fluorescence recovery, indicating that both the conjugates crossed the biological membrane (Figures 4 and 5). When compared to DFO-treated cells, $x_c$ (the fluorescence density of the majority of the cells) for both cell lines treated with **1** and **2** were significantly higher, and closer to the noniron-overloaded cells, indicating a substantial increase in cell permeability of **1** and **2** compared to the parent siderophore.

Finally, both HeLa and RBE4 cells were incubated with preformed iron complexes ([Fe] = 50 $\mu$M), and the metal levels in cells were quantified by Graphite Furnace-Atomic Absorption Spectroscopy (GF-AAS, details in the Experimental Section). In both cases, significant increase (Figure 6) in iron concentrations within the cells were observed for the iron complexes of the two conjugates, **1** and **2**, indicating that both could cross the biological membrane. In the case of HeLa cells, both iron:**1** and iron:**2** complexes showed similar cell permeability, whereas, in the case of RBE4, iron:**2** complex showed slightly better results. This agrees with our results obtained in the fluorescence assay using RBE4 cells, where conjugate **2** showed better permeability than conjugate **1**. As expected, Fe(DFO) could not enter any of the cells in a significant amount, which again proved better permeability when CPPs were used as delivery vectors.

## DISCUSSION

Growing evidence in the past decade has inarguably established that iron accumulation in certain brain areas, most probably due to genetic causes, correlates with the onset of several pathologies, viz., Alzheimer's disease (AD), Parkinson's disease (PD), or Huntington's Disease (HD), either through direct effect on amyloid-$\beta$ or $\alpha$-syn aggregation or directly due to oxidative stress.[45] Brain iron overload is the definitive feature of neurodegeneration with brain iron accumulation (NBIA) diseases.[45a] For these reasons, redox active iron in brain has been a therapeutic target for AD and other neurodegenerative diseases, and iron specific chelators have been employed for this purpose. Although DFO has shown considerable anti-Alzheimer activity,[16,23b] its low BBB permeability has forced researchers around the world to look for alternatives, albeit with less success. Our proposal toward conjugating DFO with a CPP, viz., TAT(47−57) or penetratin peptide, with proven BBB permeability, is a suitable alternative to this problem.

Toward this end, we successfully conjugated DFO with two CPPs via an N-succinyl linker while bound to a resin. This Fmoc strategy is widely employed for solid-phase peptide synthesis.[32c] All the possible pathways were explored, and the best one was employed. The synthetic route chosen was straightforward, with no practical surprises. To the best of our knowledge, no such conjugation of any iron chelator to a CPP has been reported previously. Beyond any doubt, the use of CPPs has become the most popular and efficient strategy for

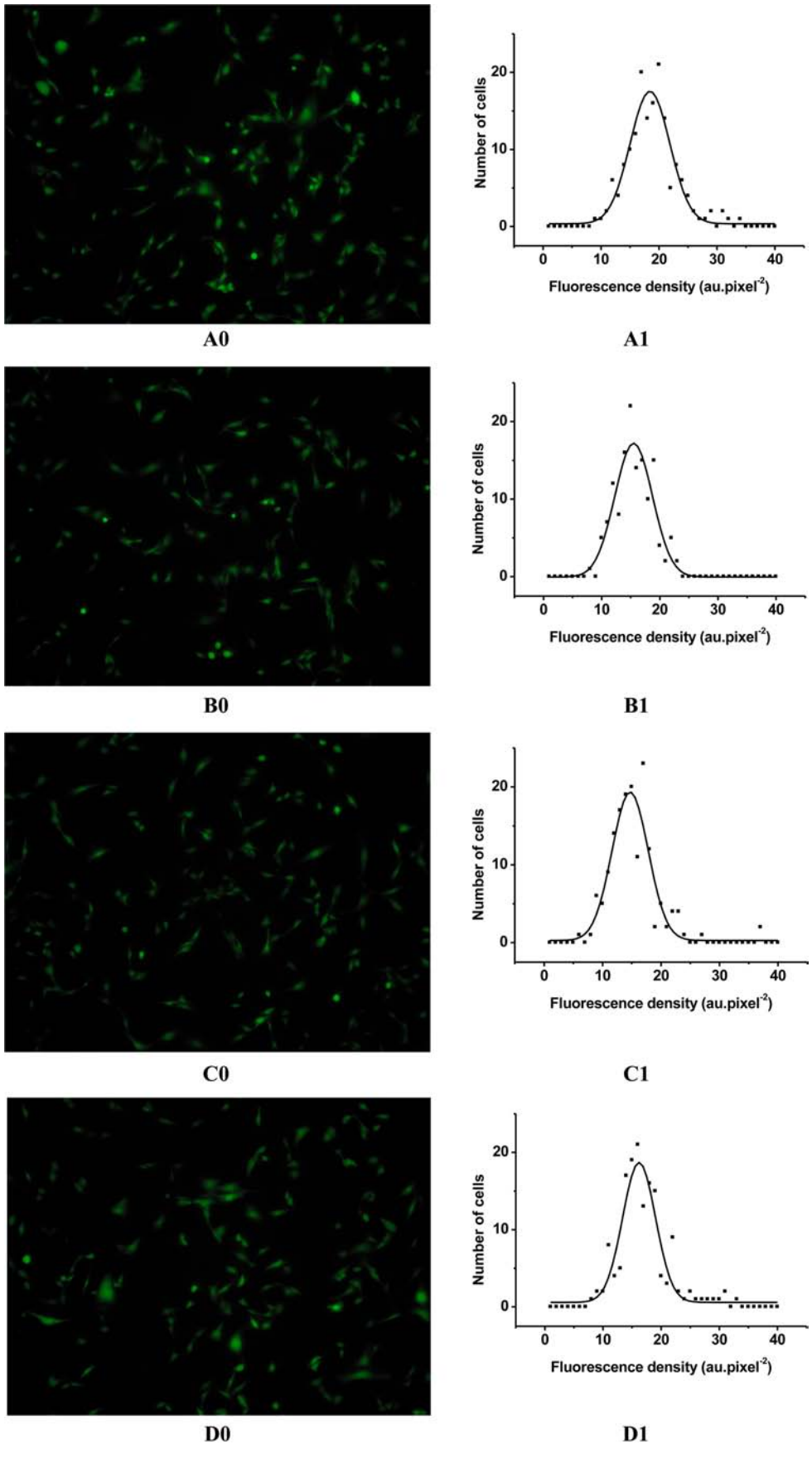


**Figure 5.** continued


dx.doi.org/10.1021/bc5004197 | *Bioconjugate Chem.* 2014, 25, 2067−2080

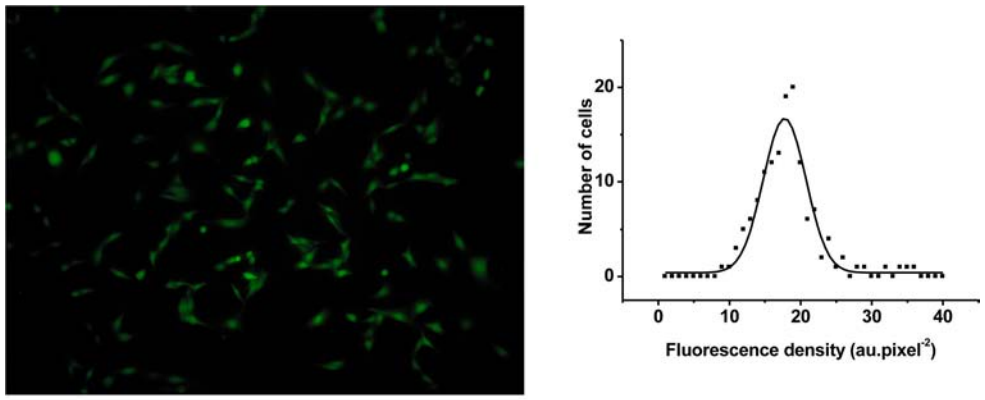


**Figure 5.** Effects of DFO, conjugate **1**, and conjugate **2** on the fluorescence of calcein in RBE4 cells. Cells were treated with buffer (A0), FAS/ascorbic acid (excess iron, B0), and excess iron plus DFO (C0), conjugate **1** (D0), or conjugate **2** (E0) (see Experimental Section). The graphs show cell population against fluorescence density for cells treated with buffer (A1, $x_c$ = 18.44 ± 0.20), after treatment with FAS/ascorbic acid (excess iron, B1, $x_c$ = 15.50 ± 0.21), and excess iron plus DFO (C1, $x_c$ = 14.72 ± 0.22), conjugate **1** (D1, $x_c$ = 16.20 ± 0.22), or conjugate **2** (E1, $x_c$ = 17.76 ± 0.16). a.u. = arbitrary fluorescence intensity.

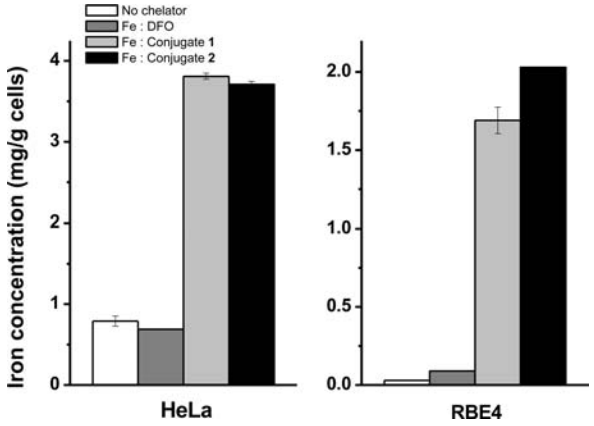


**Figure 6.** Permeability of iron:DFO or iron:**1** or iron:**2** complexes in HeLa and RBE4 cells, as measured by GF-AAS.

intracellular cargo delivery preferably using a covalent linkage between the peptide and the cargo.[46a] Several CPPs, including some target specific varieties,[46b,c] have been tested for this purpose. We have achieved a general strategy for easy coupling of the chelator moiety by conventional amide bond formation, using a succinyl linker, directly to the peptidyl-resin after completing the peptide sequence. Considering the simplicity and efficiency of our synthetic route, this strategy can be widely applied to other CPPs and be very useful.

Ideally, derivatization of an iron chelator should be such that the derivative retains chelation specificity, and presents improved properties to diminish original disadvantages. In this report, we have shown that conjugates **1** and **2** have the same iron binding abilities and antioxidant activities compared to DFO in physiologically relevant medium, and also in pHs ranging from acidic to basic. Thus, any conformational change of the peptide chain as a function of pH[47] does not have a direct impact on the iron binding of the conjugates.

Serum iron has been demonstrated as a potential target for DFO.[48] Total serum iron can be subdivided into transferrin-bound and non-transferrin-bound iron (NTBI). Our results, confirming the inability of conjugates **1** and **2**, as well as DFO, to remove iron from transferrin, corroborates the literature reports.[49] Although DFO has higher affinity for iron than transferrin, the inefficiency of the chelators to demetalate transferrin stems from kinetic factors. This is an important positive characteristic of any chelator for the treatment of iron overload, since it should remove excess iron without tampering with its proper biochemical compartments.

When Fe(NTA) was used as a model of labile iron, the rate of DHR oxidation was found to increase linearly with the concentration of Fe(NTA). In the presence of the chelators DFO, conjugate **1**, and conjugate **2**, the redox activity of the labile iron is arrested, so that the oxidation of DHR is diminished. This antioxidant property was similar to that of deferiprone, which is known[50] to have the capacity to suppress the redox activity of labile iron. These antioxidant activities of the conjugates are in synergy with their high thermodynamic affinity for iron, confirming that the conjugates form stable, redox-inactive complexes.

Although DFO has been very successful in removing labile iron from plasma, its poor membrane permeability has restricted its use for cytosolic iron overload. The results described here indicate that CPPs can be an efficient delivery vector for DFO within the cells. Throughout the years, CPPs have emerged as promising tools for cargo delivery within the cells.[26] The exact mechanism of the localization of CPPs into the cells are, however, still debated. For TAT(47−57) peptide, the basic region of the TAT protein, a recent study[51] proposed internalization via normal endocytosis after binding to heparan sulfate proteoglycans (HSPG). The same mechanism has also been proposed for small cargoes like DFO attached to TAT(47−57). In the case of penetratin, derived from the *Drosophila* antennapedia homeoprotein,[31b] however, a classical endocytosis process has been excluded.[52a,b] Alternatively, a model of translocation by interaction with membrane lipids has been proposed.[52c−e]

The use of TAT(47−57) and penetratin peptides as delivery vectors for DFO into both HeLa and RBE4 cells has proven the efficacy of the method. Both the metalated and demetalated conjugates were able to permeate through the cells, and studies have been conducted on RBE4 to explore the possibility of delivering neuropharmaceuticals to the CNS.[44] Our results proved the localization of **1** and **2** within RBE4, and also their ability to chelate iron within the cells, indicating the possibility of anti-neurodegenerative activity of both conjugates. Apart


dx.doi.org/10.1021/bc5004197 | *Bioconjugate Chem.* 2014, 25, 2067−2080

from these, recent reports[53] have indicated better gastrointestinal absorption of drugs (which are otherwise orally inactive) when coadministered with CPPs. We believe that this conjugation of DFO to CPPs can lead to better intestinal absorption of DFO, and can eventually overcome one of the major problems of DFO being orally inactive.

## CONCLUSIONS

In conclusion, we have demonstrated that the conjugation of DFO to TAT(47−57) or penetratin peptide retained the iron chelation abilities of DFO, but at the same time significantly enhanced its cell penetration efficiency. Overall, the conjugates are capable of suppressing the redox activity of iron from both buffered solutions and sera of iron-overload patients. The localization of the conjugates in RBE4 cells indicate their effectiveness as chelators in neurodegenerative diseases caused or triggered by iron overload in brain.

## EXPERIMENTAL SECTION

**Materials.** *N*-α-Fmoc-amino acids and HBTU were purchased from ChemPep Inc. (USA). Fmoc-Lys-(Boc)-Wang-resin (0.56 mmol/g) and Fmoc-Arg-(Pmc)-Wang resin (0.61 mmol/g) were purchased from Advanced Automated Peptide Protein Technologies (AAPP-TEC, USA) and Novabiochem (USA), respectively. DFO mesylate (Desferal) was donated by Novartis (USA). DIC was purchased from Advanced ChemTech (USA). HOBt was purchased from Bachem (USA). DIPEA and ninhydrin were obtained from Applied Biosystems (USA). Piperidine, TIPS, TFA, thioanisole, EDT, HEPES, NTA, FAS, ascorbic acid, calcein, calcein-AM (the cell permeant form of calcein), bovine holo-transferrin, 5-DTAF, and G418 were obtained from Sigma-Aldrich (USA). Succinic anhydride was purchased from Vetec Fine Chemicals Ltd. (Brazil). $FeCl_3$, $Fe(acac)_3$, and phenol was purchased from LabSynth (Brazil). DHR was obtained from Biotium (USA). Deferiprone was donated by Apotex. All reagents were of analytical grade and used as received without further purification. The solvents DCM and MeOH (analytical grade) were purchased from Merck (Germany), whereas DMSO (analytical grade) was obtained from Sigma-Aldrich (USA). DMF (analytical grade) and ACN (chromatographic grade) were purchased from Vetec Fine Chemicals Ltd. (Brazil). DMEM was purchased from Cultilab, Brazil. αMEM/F10 was purchased from Vitrocell (Brazil). Unless otherwise mentioned, HBS (NaCl 150 mM, HEPES 20 mM; pH 7.4; treated with Chelex-100 purchased from Sigma, 1 g/100 mL) was used throughout the experiments. Other buffer solutions used were MES (2-*N*-morpholinoethanesulfonic acid 20 mM, NaCl 150 mM; pH 5.5; treated with Chelex-100, 1 g/100 mL) and HBS 8.1 (NaCl 150 mM, HEPES 20 mM; pH 8.1; treated with Chelex-100, 1 g/100 mL).

**Peptide Purification.** Crude lyophilized peptides and peptide conjugates (synthesized according to Scheme 2) were purified by RP-HPLC using semipreparative system Model 600E consisting of a quaternary pump (Waters Delta 600 Pump), an UV detector (Waters 2487 Dual Absorbance Detector), a manual sample injector (Rheodyne 3725i-119), an automated gradient controller (Waters 600 Controller), a Kipp & Zonen recorder 124 SE, and a preparative column (Vydac C 18). The flow rate was maintained at 9.0 mL/min using 0.1% TFA/water as solvent A and 60% AcCN/0.09% TFA as solvent B. The absorbance was monitored at an wavelength of 210 nm, The following gradients were applied: 30% B to 60% B in 90 min for penetratin peptide; 10% B for 10 min, 10% B to 40% B in 75 min for TAT(47−57) peptide; 25% B to 65% B in 65 min for conjugate **1**; 20% B for 10 min, 20% B to 60% B in 80 min for conjugate **2**.

**Characterization of the Purified Peptides.** Identities of the purified peptides and conjugates were confirmed by LC/ESI−MS on a Shimadzu liquid chromatographer (Kyoto, Japan) composed of two LC-20AD pumps, a DGU-$20A_3$ degasser, a CTO-20A column oven, a C18 Shim-pack GVP-ODS precolumn, a C18 Shim-pack VP-ODS column, and SDP-20AV detector coupled to a AmaZon X electrospray mass spectrometer (Bruker Daltonics, Fahrenheitstrasse, Germany). The software HyStar 3.2 was used to analyze the mass spectra obtained. The solvents and linear gradiant used for RP-HPLC were solvent A (0.1% TFA/$H_2O$) and B (60% ACN/0.09% TFA/$H_2O$), 5% B to 95% B in 30 min.

Amino acid analysis of the purified and fully hydrolyzed peptides or conjugates (resulting from treatment with 6 M HCl at 110 °C for 24 h) was conducted in a Dionex BioLC Chromatography system (Dionex, USA) connected to an AminoPac PA10 (2.0 × 25 cm) column and the electrochemical detector ED50.

**Competition Studies with Calcein.** Aliquots of 180 μL of calcein (2 μM in HBS, pH 7.4) were placed in flat, transparent 96-well microplates and the fluorescence was recorded at 37 °C on a BMG FluoStar Optima instrument ($\lambda_{exc}/\lambda_{em}$ = 485/520 nm) for 10 min. After that, 10 μL FAS (2 μM in water, final concentration) was added to the wells, and was allowed to react at 37 °C until the fluorescence quenching was stabilized (∼10 min). The calcein-Fe (CAFe) solutions formed in the microplates were treated with increasing concentrations of the compounds under screening (10 μL aliquots), and fluorescence was further recorded until stabilization (∼60 min). To evaluate the effect of pH on this competitive equilibrium, the experiment was repeated in different buffered media, viz., MES (pH 5.5) and HBS (pH 8.1).

**Competition Studies with Fluorescein-Apotransferrin.** A sample of 180 μL of FlTf solution (2 μM in HBS, pH 7.4) was placed in flat, transparent 96-well microplates, and the fluorescence was recorded at 37 °C on a BMG FluoStar Optima instrument ($\lambda_{exc}/\lambda_{em}$ = 485/520 nm). After 10 min, the FlTf solution was loaded with 10 μL of FAS (4 μM in water, final concentration). After stabilization of fluorescence quenching (∼10 min), the solutions were treated with increasing concentrations (0−20 μM) of chelators (DFO, conjugate **1** and **2**) in 10 μL aliquots. The fluorescence was further recorded until stabilization (∼60 min).

In a second experiment designed to check whether the iron complexes of the candidate chelators were able to shuttle iron to transferrin, Iron:DFO, iron:**1**, and iron:**2** complexes (1:1 metal:ligand mol ratios) were prepared in HBS (pH 7.4, 200 μM in Fe) by incubation for 2 h at 37 °C. In this experiment, 180 μL of FlTf solutions (2 μM) were treated with increasing concentrations (0−20 μM) of the iron complexes (20 μL) as described above, and FlTf fluorescence quenching (indicating iron transfer to transferrin) was recorded.

A final experiment addressed the competition of FlTf with the chelators (DFO, **1**, and **2**) for iron. A mixture of FlTf (2 uM) with increasing concentrations (0−20 μM) of chelators (DFO, conjugates **1** and **2**) were prepared in a 96-well microplate, and FAS (10 μL, 4 uM, final concentration) was added. The changes in fluorescence were recorded as described.


dx.doi.org/10.1021/bc5004197 | *Bioconjugate Chem.* 2014, 25, 2067−2080

**Antioxidant Activity.** The standard Fe(NTA) complex (1:3 Fe:NTA molar ratio) was prepared by adding FAS to a stock solution of aqueous NTA, and allowed to react for 1 h at 37 °C. In one experiment, 180 μL of a mixture of 40 μM ascorbate and 50 μM DHR in HBS was placed in a flat, transparent 96-well microplate, and treated with 20 μL of solutions of increasing concentrations (0−10 μM) of Fe-(NTA).

In an alternative experiment, 180 μL of a mixture of 40 μM ascorbate, 50 μM DHR, and 20 μM chelators (DFO, **1**, **2**, or deferiprone) in HBS was placed in a 96-well microplate and treated with 20 μL of either Fe(NTA) at different concentrations or sera from iron overloaded patients. Assays were performed in duplicate. Sera samples were furnished by Dr. Nelson Hamerschlak, Albert Einstein Hospital, São Paulo.

Fluorescence was measured on a BMG FluoStar Optima instrument for 60 min at 37 °C ($\lambda_{exc}/\lambda_{em}$ = 485/520 nm). The slopes (indicating rate of oxidation, presented in fluorescence units per minute) of the oxidation curve were calculated in the time range 15−40 min and were plotted against chelator concentration.

**Cell Cultures.** HeLa cells were cultivated in 75 $cm^2$ cell culture flasks with DMEM containing 10% fetal bovine serum (FBS) and 1% antibiotics. RBE4 was grown in αMEM/F-10 medium containing 10% FBS, 1% antibiotics, and 300 μg/mL G418. Both cell lines were incubated at 37 °C in a humidified incubator with a 5% $CO_2$ atmosphere. Both were subcultured three times a week to prevent overcrowding and cell death.

**Fluorescence Microscopy.** Both HeLa and RBE4 cells were trypsinized and transferred ($3 \times 10^5$ cells per well) to the wells of a 6-well microplate and kept for 24 h (HeLa) or 48 h (RBE4) until complete adherence and confluence. The medium was then removed and the cells were washed with warm HBS buffer and incubated with the cell-permeant iron fluorescent probe acetomethoxycalcein (Cal-AM, 1 μM) for 10 min at 37 °C. Then, the cells were washed and treated with 1 mL of a mixture of 10 μM FAS and 100 μM ascorbic acid in water (iron-overloaded cells) or 1 mL buffer (iron-normal cells) and incubated for 15 min at 37 °C. After washing, iron-overloaded cells were treated with 20 μM chelators (DFO, **1**, or **2**) while iron-normal cells were treated with 1 mL buffer for 20 min at 37 °C. The images were obtained in an Axiovert 200 (Carl Zeiss, Germany) microscope under 100× magnification, recorded on digital camera Canon Power Shot G10, and analyzed using ImageJ 1.37c software.

**Graphite Furnace-Atomic Absorption Spectroscopy (GF-AAS) Assay.** Both HeLa and RBE4 cells were trypsinized and transferred ($3 \times 10^5$ cells per well) to the plates of a 6-well microplate and kept for 24 h (HeLa) or 48 h (RBE4) until complete adherence and confluence. The medium was then removed and the cells were washed with warm HBS buffer. Cells were then incubated with 1 mL HBS (control group) or 1 mL of preformed iron:DFO, iron:**1**, or iron:**2** complexes ([Fe] = 50 μM) in HBS for 30 min at 37 °C. Cells were washed (1 × 1 mL HBS; 2 × 1 mL DFO 100 μM in HBS) to remove any unbound iron left, and were dried under vacuum.

Determination of Fe concentration in each well was performed with a ZEEnit 60, Analytikjena AG (Jena, Germany) graphite furnace atomic absorption spectrometer equipped with a two-field mode Zeeman effect background corrector, integrated platform graphite tube atomizer, and a hollow cathode lamp (wavelength = 248.3 nm, slit width = 0.8 nm, and lamp current = 4.0 mA). Calibration curves were obtained by using aqueous standard solutions. Cells samples were digested by adding 300 μL of $HNO_3$ (65% v/v) and 100 μL $H_2O_2$ (30% v/v) to 0.4 mg of cell samples which were heated to 100 °C for 5 min. The volume was adjusted to 2 mL using deionized water. The heating program used for iron measurement was (step: temperature, °C/ramp (°C/s)/hold (s)): (drying 1:100, 10, 15); (drying 2:130, 10, 20); (pyrolysis: 1000, 100, 20); (atomization: 2200, 2600, 5), and (cleaning: 2500, 1200, 5).

## ■ ASSOCIATED CONTENT

### Supporting Information

LC-MS and analytical HPLC of TAT(47−57), Penetratin, conjugate **1** and conjugate **2**. This material is available free of charge via the Internet at http://pubs.acs.org.

## ■ AUTHOR INFORMATION

### Corresponding Author

*E-mail: breno@iq.usp.br; Phone: + 55 11 3091 9141; fax: + 55 11 3815 5579.

### Notes

The authors declare no competing financial interest.

## ■ ACKNOWLEDGMENTS

This work was supported by FAPESP and CNPq (Brazilian government agencies). D.G. received a postdoctoral grant from FAPESP, and D.M.S. received doctoral fellowship from CNPq. The authors thank Prof. Mauricio S. Baptista and Dr. Cleber Wanderlei Liria for discussions and technical assistance.

## ■ ABBREVIATIONS

HBTU, 2-(1*H*-benzotriazole-1-yl)-1,1,3,3-tetramethyluronium hexafluorophosphate; DIC, *N,N′*-diisopropylcarbodiimide; HOBt, *N*-hydroxybenzotriazole; DIPEA, diisopropylamine; TIPS, triisopropylsilane; TFA, trifluoroacetic acid; EDT, ethanedithiol; PhOH, phenol; DCM, dichloromethane; MeOH, methanol; DMSO, dimethyl sulfoxide; DMF, *N,N′*-dimethylformamide; ACN, acetonitrile; NTA, nitrilotriacetic acid; FAS, ferrous ammonium sulfate; HBS, HEPES buffered saline; acac, acetylacetonate; 5-DTAF, 5-(4,6-dichlorotriazinyl)-aminofluorescein; DHR, dihydrorhodamine hydrochloride; DMEM, Dulbecco's Modified Eagle Medium; αMEM/F-10, Alpha Minimum Eagle Medium 1:1 Ham's F10 Medium

## ■ REFERENCES

(1) McDowell, L. R. (2003) Iron. *Minerals in Animal And Human Nutrition*, 2nd ed., pp 203−233, Chapter 7, Elsevier Science, Amsterdam.

(2) Abbaspour, N., Hurrell, R., and Kelishadi, R. (2014) Review on iron and its importance for human health. *J. Res. Med. Sci. 19*, 164−174.

(3) Piperno, A. (1998) Classification and diagnosis of iron overload. *Haematologica 83*, 447−455.

(4) (a) Breuer, W., Epsztejn, S., and Cabantchik, Z. I. (1996) Dynamics of the cytosolic chelatable iron pool of K562 cells. *FEBS Lett. 382*, 304−308. (b) Cabantchik, Z. I., Breuer, W., Zanninelli, G., and Cianciulli, P. (2005) LPI-labile plasma iron in iron overload. *Best Pract. Res., Clin. Haematol. 18*, 277−287.

(5) Halliwell, B., and Gutteridge, J. M. C. (1989) *Free Radicals in Biology and Medicine*, 2nd ed., pp 63, Oxford University Press, Oxford.

(6) (a) Aisen, P., Enns, C., and Wessling-Resnick, M. (2001) Chemistry and biology of eukaryotic iron metabolism. *Int. J. Biochem. Cell B 33*, 940−959. (b) Sebastiani, G., and Pantopoulos, K. (2011) Disorders associated with systemic or local iron overload: from pathophysiology to clinical practice. *Metallomics 3*, 971−986.

(c) Fleming, R. E., and Ponka, P. (2012) Mechanisms of disease: iron overload in human disease. *N. Engl. J. Med. 366*, 348−59.
(7) Barnham, K. J., Masters, C. L., and Bush, A. I. (2004) Neurodegenerative diseases and oxidative stress. *Nat. Rev. Drug Discovery 3*, 205−214.
(8) (a) Zecca, L., Youdim, M. B. H., Riederer, P., Connor, J. R., and Crichton, R. R. (2004) Iron, brain ageing and neurodegenerative disorders. *Nat. Rev. Neurosci. 5*, 863−873. (b) Halliwell, B. (2006) Oxidative stress and neurodegeneration: where are we now? *J. Neurochem. 97*, 1634−1658. (c) Piloni, N. E., Fermandez, V., Videla, L. A., and Puntarulo, S. (2013) Acute iron overload and oxidative stress in brain. *Toxicology 314*, 174−182.
(9) (a) Raven, E. P., Lu, P. H., Heydari, T. A. P., and Bartzokis, G. (2013) Increased iron levels and decreased tissue integrity in hippocampus of Alzheimer's disease detected in vivo with magnetic resonance imaging. *J. Alzheimer's Dis. 37*, 127−136. (b) Bartzokis, G., Cummings, J. L., Markham, C. H., Marmarelis, P. Z., Treciokas, L. J., Tishler, T. A., Marder, S. R., and Mintz, J. (1999) MRI evaluation of brain iron in earlier- and later-onset Parkinson's disease and normal subjects. *Magn. Reson. Imaging 17*, 213−222. (c) Hadzhieva, M., Kirches, E., and Mawrin, C. (2014) Review: Iron metabolism and the role of iron in neurodegenerative disorders. *Neuropathol. Appl. Neurobiol. 40*, 240−257. (d) Bartzokis, G., and Tishler, T. A. (2000) MRI evaluation of basal ganglia ferritin iron and eurotoxicity in Alzheimer's and Huntingon's disease. *Cell Mol. Biol. 46*, 821−833. (e) Bartzokis, G., Lu, P. H., Tingus, K., Peters, D. G., Amar, C. P., Tishler, T. A., Finn, J. P., Villablanca, P., Altshuler, L. L., Mintz, J., Neely, E., and Connor, J. R. (2011) Gender and iron genes may modify associations between brain iron and memory in healthy aging. *Neuropsychopharmacology 36*, 1375−1384.
(10) (a) Bondy, S. C., Guo-Ross, S. X., and Truong, A. T. (1998) Promotion of transition metal-induced reactive oxygen species formation by *β*-amyloid. *Brain Res. 799*, 91−96. (b) Lovell, M. A., Robertson, J. D., Teesdale, W. J., Campbell, J. L., and Markesbery, W. R. (1998) Copper, iron and zinc in Alzheimer's disease senile plaques. *J. Neurol. Sci. 158*, 47−52. (c) Bush, A. I., Pettingell, W. H., Multhaup, G., Paradis, M. D., Vonsattel, J. P., Gusella, J. F., Beyreuther, K., Masters, C. L., and Tanzi, R. E. (1994) Rapid induction of Alzheimer A beta amyloid formation by zinc. *Science 265*, 1464−1467. (d) Liu, G., Men, P., Perry, G., and Smith, M. A. (2010) Nanoparticle and iron chelators as a potential novel Alzheimer therapy. *Methods Mol. Biol. 610*, 123−144.
(11) (a) Kalinowski, D. S., and Richardson, D. R. (2005) The evolution of iron chelators for the treatment of iron overload disease and cancer. *Pharmacol. Rev. 57*, 547−583. (b) Dixon, S. J., and Stockwell, B. R. (2014) The role of iron and reactive oxygen species in cell death. *Nat. Chem. Biol. 10*, 9−17.
(12) (a) Hider, R. C., and Hall, A. D. (1991) 2 clinically useful chelators of tripositive elements. *Prog. Med. Chem. 28*, 41−173. (b) Bendova, P., Mackova, E., Haskova, P., Vavrova, A., Jirkovsky, E., Sterba, M., Popelova, O., Kalinowski, D. S., Kovarikova, P., Vavrova, K., Richardson, D. R., and Simunek, T. (2010) Comparison of clinically used and experimental iron chelators for protection against oxidative stress-induced cellular injury. *Chem. Res. Toxicol. 23*, 1105−1114.
(13) (a) Aouad, F., Florence, A., Zhang, Y., Collins, F., Henry, C., Ward, R. J., and Crichton, R. R. (2002) Evaluation of new iron chelators and their therapeutic potential. *Inorg. Chim. Acta 339*, 470−480. (b) Brittenham, G. M. (2003) Iron chelators and iron toxicity. *Alcohol 30*, 151−158.
(14) (a) Olivieri, N. F., and Brittenham, G. M. (1997) Iron-chelating therapy and the treatment of thalassemia. *Blood 89*, 739−761. (b) Blatt, J., and Stitely, S. (1987) Antineuroblastoma activity of desferoxamine in human cell lines. *Cancer Res. 47*, 1749−1750.
(15) Sharma, R. N., and Pancholi, S. S. (2010) Oral iron chelators: a new avenue for the management of thalassemia major. *J. Curr. Pharm. Res. 1*, 1−7 , and the references cited therein..
(16) McLachlan, D. R., Kruck, T. P., Lukiw, W. J., and Krishnan, S. S. (1991) Would decreased aluminum ingestion reduce the incidence of Alzheimer's disease? *Can. Med. Assoc. J. 145*, 793−804.
(17) Lynch, S. G., Fonseca, T., and Levine, S. (2000) A multiple course trial of desferrioxamine in chronic progressive multiple sclerosis. *Cell Mol. Biol. 46*, 865−869.
(18) Liu, G., Men, P., Perry, G., and Smith, M. A. (2009) Chapter 5-Development of iron chelator−nanoparticle conjugates as potential therapeutic agents for Alzheimer disease. *Prog. Brain Res. 180*, 97−108.
(19) (a) Liu, X. S., Patterson, L. D., Miller, M. J., and Theil, E. C. (2007) Peptides selected for the protein nanocage pores change the rate of iron recovery from the ferritin mineral. *J. Biol. Chem. 282*, 31821−31825. (b) Moggia, F., Brisset, H., Fages, F., Chaix, C., Mandrand, B., Dias, M., and Levillain, E. (2006) Design, synthesis and redox properties of two ferrocene-containing iron chelators. *Tetrahedron Lett. 47*, 3371−3374. (c) Loyevsky, M., Lytton, S. D., Mester, B., Libman, J., Shanzer, A., and Cabantchik, Z. I. (1993) The antimalarial action of Desferal involves a direct access route to erythrocytic (Plasmodium falciparum) parasites. *J. Clin. Invest. 91*, 218−224. (d) Palanch_e, T., Marmolle, F., Abdallah, M. A., Shanzer, A., and Albrecht-Gary, A.-M. (1999) Fluorescent siderophore-based chemosensors: iron(III) quantitiative determinations. *J. Biol. Inorg. Chem. 4*, 188−198. (e) Ghosh, M., Lambert, L. J., Huber, P. W., and Miller, M. J. (1995) Synthesis, bioactivity, and DNA-cleaving ability of Desferrioxamine B-nalidixic acid and Anthraquinone carboxylic acid conjugates. *Bioorg. Med. Chem. Lett. 5*, 2337−2340. (f) Hou, Z., Whisenhunt, D. W. J., Xu, J., and Raymond, K. N. (1994) Potentiometric, spectrophotometric, and $^{1}$H NMR study of four Desferrioxamine B derivatives and their ferric complexes. *J. Am. Chem. Soc. 116*, 840−846. (g) Rodgers, S. J., and Raymond, K. N. (1983) Ferric ion sequestering agents. 11. Synthesis and kinetics of iron removal from transferrin of catechoyl derivatives of Desferrioxamine B. *J. Med. Chem. 26*, 439−442. (h) White, D. L., Durbin, P. W., Jeung, N., and Raymond, K. N. (1988) Specific sequestering agents from the actinites. 16. Synthesis and initial biological testing of polydentate Oxohydroxypyridinecarboxylate ligands. *J. Med. Chem. 31*, 11−18. (i) Liu, J., Obando, D., Schipanski, L. G., Groebler, L. K., Witting, P. K., Kalinowski, D. S., Richardson, D. R., and Codd, R. (2010) Conjugates of Desferrioxamine B (DFOB) with derivatives of adamantane or with orally available chelators as potential agents for treating iron overload. *J. Med. Chem. 53*, 1370−1382. (j) Liddell, J. R., Obando, D., Liu, J., Ganio, G., Volitakis, I., Mok, S. S., Crouch, P. J., White, A. R., and Codd, R. (2013) Lipophilic adamantyl- or deferasirox-based conjugates of desferrioxamine B have enhanced neuroprotective capacity: implications for Parkinson disease. *Free Radic. Biol. Med. 60*, 147−156. (k) Dragsten, P. R., Hallaway, P. E., Hanson, G. J., Berger, A. E., Bernard, B., and Hedlund, B. E. (2000) First human studies with a high-molecular-weight iron chelator. *J. Lab. Clin. Med. 135*, 57−65. (l) Poreddy, A. R., Schall, O. F., Osiek, T. A., Wheatley, J. R., Beusen, D. D., Marshall, G. R., and Slomczynska, U. (2004) Hydroxamate-based iron chelators: combinatorial syntheses of desferrioxamine B analogues and evaluation of binding affinities. *J. Comb. Chem. 6*, 239−254.
(20) (a) Huang, X., Moir, R. D., Tanzi, R. E., Bush, A. I., and Rogers, J. T. (2004) Redox-active metals, oxidative stress, and Alzheimer's disease pathology. *Ann. N.Y. Acad. Sci. 1012*, 153−163. (b) Amit, T., Avramovich-Tirosh, Y., Youdim, M. B. H., and Mandel, S. (2008) Targeting multiple Alzheimer's disease etiologies with multimodal neuroprotective and neurorestorative iron chelators. *FASEB J. 22*, 1296−1305. (c) Wang, Y., Branicky, R., Stepanyan, Z., Carroll, M., Guimond, M.-P., Hihi, A., Hayes, S., McBride, K., and Hekimi, S. (2009) The anti-neurodegeneration drug clioquinol inhibits the aging-associated protein CLK-1. *J. Biol. Chem. 284*, 314−323.
(21) Yuan, J., Loveyoy, D. B., and Richardson, D. R. (2004) Novel di-2-pyridyl−derived iron chelators with marked and selective antitumor activity: in vitro and in vivo assessment. *Blood 104*, 1450−1458.
(22) Scott, L. E., and Orvig, C. (2009) Medicinal inorganic chemistry approaches to passivation and removal of aberrant metal ions in disease. *Chem. Rev. 109*, 4885−4910.

(23) (a) Youdim, M. B. H., Fridkin, M., and Zheng, H. (2004) Novel bifunctional drugs targeting monoamine oxidase inhibition and iron chelation as an approach to neuroprotection in Parkinson's disease and other neurodegenerative diseases. *J. Neural Transm. Suppl. 71*, 163−172. (b) Perez, C. A., Tong, Y., and Guo, M. (2008) Iron chelators as potential therapeutic agents for Parkinsons disease. *Curr. Bioact. Compd. 4*, 150−158.

(24) Liu, Z. D., and Hider, R. C. (2002) Iron chelator chemistry. In *Molecular and Cellular Iron Transport* (Templeton, D., Ed.) p 360, CRC Press, New York.

(25) Hider, R. C., Porter, J. B., and Singh, S. (1994) The design of therapeutically useful iron chelators. In *The development of iron chelators for clinical use* (Bergeron, R. J., and Brittenham, G. M., Eds.) pp 353−371, CRC Press, Boca Raton.

(26) (a) Copolovici, D. M., Langel, K., Eriste, E., and Langel, Ü. (2014) Cell-penetrating peptides: design, synthesis, and applications. *ACS Nano 8*, 1972−1994. (b) Brooks, H., Lebleu, B., and Vives, E. (2005) Tat peptide-mediated cellular delivery: back to basics. *Adv. Drug Delivery Rev. 57*, 559−577. (c) Majumdar, S., and Siahaan, T. J. (2012) Peptide-mediated targeted drug delivery. *Med. Res. Rev. 32*, 637−658. (d) Wang, F., Wang, Y., Zhang, X., Zhang, W., Guo, S., and Jin, F. (2014) Recent progress of cell-penetrating peptides as new carriers for intracellular cargo delivery. *J. Controlled Release 174*, 126−136. (e) León-Rodríguez, L. M. D., and Kovacs, Z. (2008) The synthesis and chelation chemistry of DOTA-peptide conjugates. *Bioconjugate Chem. 19*, 391−402.

(27) Heitz, F., Morris, M. C., and Divita, G. (2009) Twenty years of cell-penetrating peptides: from molecular mechanisms to therapeutics. *Br. J. Pharmacol. 157*, 195−206.

(28) (a) Frankel, A. D., and Pabo, C. O. (1988) Cellular uptake of the Tat protein from human immunodeficiency virus. *Cell 55*, 1189−1193. (b) Green, M., and Loewenstein, P. M. (1988) Autonomous functional domains of chemically synthesized human immunodeficiency virus Tat trans-activator protein. *Cell 55*, 1179−1188.

(29) Derossi, D., Joliot, A. H., Chassaing, G., and Prochiantz, A. (1994) The third helix of the Antennapedia homeodomain translocates through biological membranes. *J. Biol. Chem. 269*, 10444−10450.

(30) (a) Schwarze, S. R., Ho, A., Vocero-Akbani, A., and Dowdy, S. F. (1999) In vivo protein transduction: delivery of a biologically active protein into the mouse. *Science 285*, 1569−1572. (b) Qin, Y., Chen, H., Yuan, W., Kuai, R., Zhang, Q., Xie, F., Zhang, L., Zhang, Z., Liu, J., and He, Q. (2011) Liposome formulated with TAT- modified cholesterol for enhancing the brain delivery. *Int. J. Pharm. 419*, 85−95. (c) Liu, L., Venkatraman, S. S., Yang, Y.-Y., Guo, K., Lu, J., He, B., Moochhala, S., and Kan, L. (2008) Polymeric micelles anchored with TAT for delivery of antibiotics across the blood-brain barrier. *Biopolymers 90*, 617−23. (d) Wadia, J. S., Stan, R. V., and Dowdy, S. F. (2004) Transducible TAT-HA fusogenic peptide enhances escape of TAT-fusion proteins after lipid raft macropinocytosis. *Nat. Med. 10*, 310−315. (e) Torchilin, V. P., Rammohan, R., Weissig, V., and Levchenko, T. S. (2001) TAT peptide on the surface of liposomes affords their efficient intracellular delivery even at low temperature and in the presence of metabolic inhibitors. *Proc. Natl. Acad. Sci. U. S. A. 98*, 8786−8791.

(31) (a) Dupont, E., Prochiantz, A., and Joliot, A. (2006) Penetratins. In *Handbook of cell penetrating peptides*, 2nd ed. (Langel, Ü., Ed.) pp 5−28, CRC Press, Boca Raton. (b) Rousselle, C., Clair, P., Lefauconnier, J. M., Kaczorek, M., Scherrmann, J. M., and Temsamani, J. (2000) New advances in the transport of doxorubicin through the blood-brain barrier by a peptide vector-mediated strategy. *Mol. Pharmacol. 57*, 679−686. (c) Bolton, S. J., Jones, D. N., Darker, J. G., Eggleston, D. S., Hunter, A. J., and Walsh, F. S. (2000) Cellular uptake and spread of the cell-permeable peptide penetratin in adult rat brain. *Eur. J. Neurosci. 12*, 2847−2855.

(32) (a) Souza, M. P., Tavares, M. F. M., and Miranda, M. T. M. (2004) Racemization in stepwise solid-phase synthesis at elevated temperatures. *Tetrahedron 60*, 4671−4681. (b) Remuzgo, C., Andrade, G. F. S., Temperini, M. L. A., and Miranda, M. T. M. (2009) Acanthoscurrin fragment 101−132: total synthesis at 60°C of a novel difficult sequence. *Biopolymers (Pept. Sci.) 92*, 65−75. (c) Loffredo, C., Assunção, N. A., Gerhardt, J., and Miranda, M. T. M. (2009) Microwave-assisted solid-phase peptide synthesis at 60°C: alternative conditions with low enantiomerization. *J. Pept. Sci. 15*, 808−815.

(33) Kaiser, E., Colescott, R. L., Bossinger, C. D., and Cook, P. I. (1970) Color test of detection of free amino groups in the solid phase synthesis of peptides. *Anal. Biochem. 34*, 595−598.

(34) Adapa, S., Huher, P., and Keller-Schierlein, W. (1982) Isolierung, strukturaufklarung und synthese von ferrioxamin H. *Helv. Chim. Acta 65*, 1818−1824.

(35) Prelog, V. (1963) Iron-containing antibiotics and microbic growth factors. *Pure Appl. Chem. 6*, 327−338.

(36) Kline, M. A., and Orvig, C. (1992) Complexation of iron with the orally active decorporation drug L1 (3-Hydroxy-1,2-dimethyl-4-pyridinone). *Clin. Chem. 38*, 562−565.

(37) Hsieh, H.-P., Wu, Y.-T., Chen, S.-T., and Wang, K.-T. (1999) Direct solid-phase synthesis of octreotide conjugates: precursors for use as tumor-targeted radiopharmaceuticals. *Bioorg. Med. Chem. 7*, 1797−1803.

(38) Kiyota, S., Franzoni, L., Nicastro, G., Benedetti, A., Oyama, S. JR., Viviani, W., Gambarini, A. G., Spisni, A., and Miranda, M. T. (2003) Introduction of a chemical constraint in a short peptide derived from human acidic fibroblast growth factor licits mitogenic structural determinants. *J. Med. Chem. 46*, 2325−2333.

(39) (a) Thomas, F., Serratrice, G., Béguin, C., Aman, E. S., Pierre, J. L., Fontecave, M., and Laulhère, J. P. (1999) Calcein as a fluorescent probe for ferric iron: application to iron nutrition in plant cells. *J. Biol. Chem. 274*, 13375−13383. (b) Espósito, B. P., Epsztejn, S., Breuer, W., and Cabantchik, Z. I. (2002) A review of fluorescence methods for assessing labile iron in cells and biological fluids. *Anal. Biochem. 304*, 1−18. (c) Breuer, W., Epsztejn, S., and Cabantchik, Z. I. (1995) Iron acquired from transferrin by K562 cells Is delivered into a cytoplasmic pool of chelatable iron(II). *J. Biol. Chem. 270*, 24209−24215.

(40) (a) Martin, R. B., Savory, J., Brown, S., Bertholf, R. L., and Wills, M. R. (1987) Transferrin binding of $Al^{3+}$ and $Fe^{3+}$. *Clin. Chem. 33*, 405−407. (b) Turcot, I., Stintzi, A., Xu, J., and Raymond, K. N. (2000) Fast biological iron chelators: kinetics of iron removal from human diferric transferrin by multidentate hydroxypyridonates. *J. Biol. Inorg. Chem. 5*, 634−641.

(41) Breuer, W., and Cabantchik, Z. I. (2001) A fluorescence-based one-step assay for serum non-transferrin-bound iron. *Anal. Biochem. 299*, 194−202.

(42) Espósito, B. P., Breuer, W., Sirankapracha, P., Hershko, C., and Cabantchik, Z. I. (2003) Labile plasma iron in iron overload: redox activity and susceptibility to chelation. *Blood 102*, 2670−2677.

(43) Gomes, A., Fernandes, E., and Lima, J. L. F. C. (2005) Fluorescence probes used for detection of reactive oxygen species. *J. Biochem. Biophys. Methods. 65*, 45−80 , and the references cited therein.

(44) (a) Wilhelm, I., Fazakas, C., and Krizbai, I. A. (2011) In vitro models of the blood- brain barrier. *Acta Neurobiol. Exp. 71*, 113−128. , and the references cited therein. (b) Reichel, A., Abbot, N. J., and Begley, D. J. (2002) Evaluation of the RBE4 cell line to explore carrier-mediated drug delivery to the CNS via the L-system amino acid transporter at the blood-brain barrier. *J. Drug Targeting 10*, 277−283.

(45) (a) Rouault, T. A. (2013) Iron metabolism in the CNS: implications for neurodegenerative diseases. *Nat. Rev. Neurosci. 14*, 551−564. Batista-Nascimento, L., Pimentel, C., Menezes, R. A., and Rodrigues-Pousada, C. (2012) Iron and neurodegeneration: from cellular homeostasis to disease. *Oxid. Med. Cell Longev.*, 128647 DOI: 10.1155/2012/128647. (c) Thompson, K. J., Shoham, S., and Connor, J. R. (2001) Iron and neurodegenerative disorders. *Brain Res. Bull. 55*, 155−164.

(46) (a) Johnson, R. M., Harrison, S. D., and Maclean, D. (2011) Therapeutic applications of cell-penetrating peptides. *Methods Mol. Biol. 683*, 535−551. (b) Shi, N.-Q., Gao, W., Xiang, B., and Qi, X.-R. (2012) Enhancing cellular uptake of activable cell-penetrating peptide−doxorubicin conjugate by enzymatic cleavage. *Int. J. Nano-*

*medicine 7*, 1613−1621. (c) Lim, K. J., Sung, B. H., Shin, J. R., Lee, Y. W., Kim, D. J., Yang, K. S., and Kim, S. C. (2013) A cancer specific cell-penetrating peptide, BR2, for the efficient delivery of an scFv into cancer cells. *PLoS One 8*, e66084.

(47) (a) Wang, W., Nema, S., and Teagarden, D. (2010) Protein aggregation-pathways and influencing factors. *Int. J. Pharm. 390*, 89−99. (b) Pagel, K., Wagner, S. C., Samedov, K., vonBerlepsch, H., Böttcher, C., and Koksch, B. (2006) Random coils, $\beta$-sheet ribbons, and $\alpha$-helical fibers: one peptide adopting three different secondary structures at will. *J. Am. Chem. Soc. 128*, 2196−2197. (c) Mahler, H.-C., Friess, W., Grauschopf, U., and Kiese, S. (2009) Protein aggregation: pathways, induction factors and analysis. *J. Pharm. Sci. 98*, 2909−2934.

(48) Breuer, W., Ermers, M. J. J., Pootrakul, P., Abramov, A., Hershko, C., and Cabantchik, Z. I. (2001) Desferrioxamine-chelatable iron, a component of serum non−transferrin-bound iron, used for assessing chelation therapy. *Blood 97*, 792−798.

(49) Pollack, S., Vanderhoff, G., and Lasky, F. (1977) Iron removal from transferrin-an experimental study. *Biochim. Biophys. Acta 497*, 481−487.

(50) Kontoghiorghes, G. J. (2009) Prospects for introducing deferiprone as potent pharmaceutical antioxidant. *Front. Biosci. (Elite Ed) 1*, 161−178.

(51) Mishra, A., Lai, G. H., Schmidt, N. W., Sun, V. Z., Rodriguez, A. R., Tong, R., Tang, L., Cheng, J., Deming, T. J., Kamei, D. T., and Wong, G. C. L. (2011) Translocation of HIV TAT peptide and analogues induced by multiplexed membrane and cytoskeletal interactions. *Proc. Natl. Acad. Sci. U.S.A. 108*, 16883−16888.

(52) (a) Derossi, D., Calvet, S., Trembleau, A., Brunissen, A., Chassaing, G., and Prochiantz, A. (1996) Cell internalization of the third helix of the Antennapedia homeodomain is receptor-independent. *J. Biol. Chem. 271*, 18188−18193. (b) Fischer, P. M., Zhelev, N. Z., Wang, S., Melville, J. E., Fåhraeus, R., and Lane, D. P. (2000) Structure−activity relationship of truncated and substituted analogues of the intracellular delivery vector Penetratin. *J. Pept. Res. 55*, 163−172. (c) Berlose, J.-P., Convert, O., Derossi, D., Brunissen, A., and Chassaing, G. (1996) Conformational and associative behaviours of the third helix of Antennapedia homeodomain in membrane-mimetic environments. *Eur. J. Biochem. 242*, 372−386. (d) Prochiantz, A. (1996) Getting hydrophilic compounds into cells: lessons from homeopeptides. *Curr. Opin. Neurobiol. 6*, 629−634. (e) Thorén, P. E. G., Persson, D., Karlsson, M., and Nordén, B. (2000) The Antennapedia peptide penetratin translocates across lipid bilayers−the first direct observation. *FEBS Lett. 482*, 265−268.

(53) Kamei, N., Morishita, M., Eda, Y., Ida, N., Nishio, R., and Takayama, K. (2008) Usefulness of cell-penetrating peptides to improve intestinal insulin absorption. *J. Controlled Release 132*, 21−25 , and references cited therein.